European Journal of Medicinal Chemistry 221 (2021) 113545

Contents lists available at ScienceDirect

European Journal of Medicinal Chemistry

journal homepage: http://www.elsevier.com/locate/ejmech

Synthesis, *in vitro* antiprotozoal activity, molecular docking and molecular dynamics studies of some new monocationic guanidinobenzimidazoles

Fatima Doganc [a], Ismail Celik [b], Gokcen Eren [c], Marcel Kaiser [d, e], Reto Brun [d, e], Hakan Goker [a, *]

[a] Department of Pharmaceutical Chemistry, Faculty of Pharmacy, Ankara University, 06100, Tandogan, Ankara, Turkey
[b] Department of Pharmaceutical Chemistry, Faculty of Pharmacy, Erciyes University, 38280, Yenidogan, Kayseri, Turkey
[c] Department of Pharmaceutical Chemistry, Faculty of Pharmacy, Gazi University, 06330, Etiler, Ankara, Turkey
[d] Parasite Chemotherapy Unit, Swiss Tropical and Public Health Institute, Basel, CH, 4002, Switzerland
[e] University of Basel, Basel, CH, 4001, Switzerland

ARTICLE INFO

Article history:
Received 10 March 2021
Received in revised form
7 May 2021
Accepted 8 May 2021
Available online 24 May 2021

Keywords:
Antiparasitic activity
Molecular docking
Molecular dynamics
Monocationic guanidinobenzimidazoles

ABSTRACT

A series of monocationic new guanidinobenzimidazole derivatives were prepared in a four step process starting from 2-nitro-1,4-phenylendiamine. Their antiparasitic activity against *Plasmodium falciparum*, *Trypanosoma brucei rhodesiense*, *Trypanosoma cruzi* and *Leishmania donovani* were evaluated *in vitro*. Two out of 20 tested monocationic compounds **(7, 14)** showed close activity with reference drug chloroquine against *P. Falciparum*. To understand the interactions between DNA minor groove and *in vitro* active compounds **(7, 14)** molecular docking studies were carried out. Stability and binding energies of DNA-ligand complexes formed by DNA with compounds **7** and **14** were measured by molecular dynamics simulations throughout 200 ns time. Root mean square deviation (RMSD) values of the ligands remained stable below 0.25 mm and root mean square fluctuation (RMSF) values of the active site residues with which it interacted decreased compared to the apo form. All compounds exhibited theoretical absorption, distribution, metabolism and excretion (ADME) profiles conforming to Lipinski's and Ghose's restrictive rules.

© 2021 Elsevier Masson SAS. All rights reserved.

1. Introduction

Neglected tropical diseases (NTDs) are a diverse group of infectious diseases common in 149 countries especially in tropical and subtropical regions, affecting more than 1 billion people each year [1]. Parasitic infections are common even in developing countries and cause important opportunistic infections, particularly in immunocompromised patients. Among them, malaria, sleeping sickness (Human Africa Trypanosomiasis, HAT), Chagas disease and leishmaniasis are responsible for a considerable amount of human mortality, morbidity and economic hardship [2,3]. Protozoan parasites are resistant to a large number of drugs. In addition, drugs used in the treatment are highly toxic and have long treatment periods and significant side effects. Also, cost related problems and lack of oral bioavailability reveal the requirement for the development of new antiparasitic compounds [3].

Aromatic amidine derivatives are known as a group of compounds that interact with DNA. These compounds show *in vitro* antiprotozoal activity by binding to the DNA minor groove, especially AT base pairs. These derivatives have been used for years in the treatment of protozoal diseases. Pentamidine (Fig. 1) is a compound used clinically in the treatment of sleeping sickness and antimony-resistant leishmaniasis [4,5]. But, it is not effective when given orally and various toxic effects such as hypotension, dysglycemia, kidney and liver toxicity have been reported [6].

Until today, based on pentamidine, many similar analogues and new derivatives with different cationic and heterocyclic structures have been synthesized and antiprotozoal activities have been screened. Among these, furamidine has lower toxicity and

Abbreviations: NTDs, Neglected tropical diseases; RMSD, Root mean square deviation; RMSF, Root mean square fluctuation; TMS, Tetra methyl silane; VMD, Visual molecular dynamics.

* Corresponding author.
E-mail address: goker@ankara.edu.tr (H. Goker).

https://doi.org/10.1016/j.ejmech.2021.113545
0223-5234/© 2021 Elsevier Masson SAS. All rights reserved.

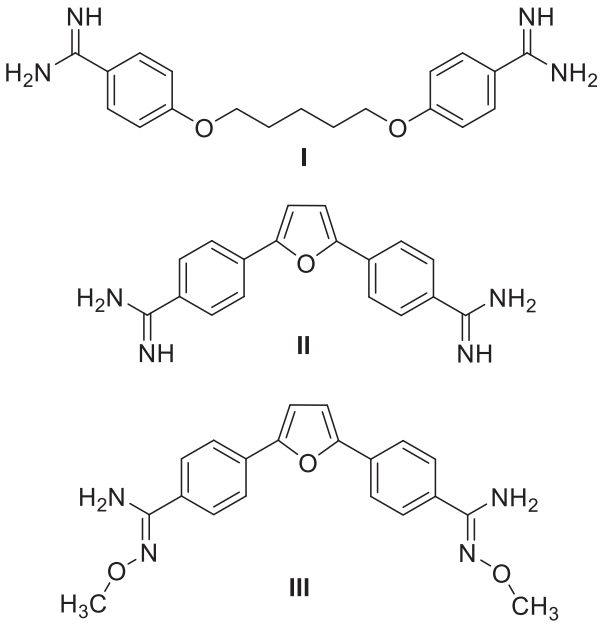

Fig. 1. Pentamidine **(I)**, Furamidine **(II)** and Pafuramidine **(III)**.

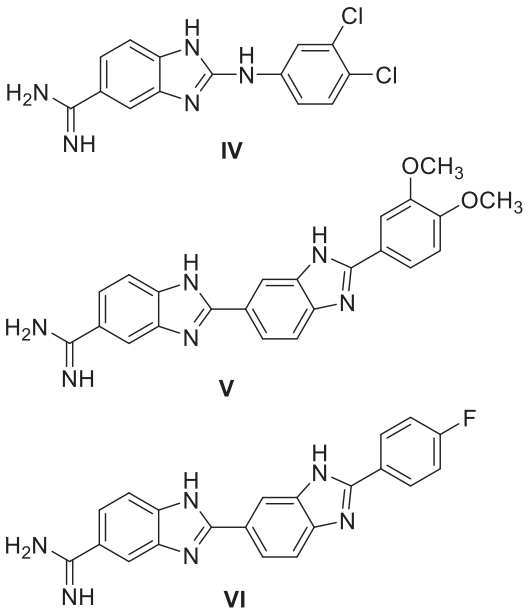

Fig. 3. The structures of previously reported monocationic compounds possessing potent antiprotozoal activity.

remarkably better activity against protozoan parasites than pentamidine. Furamidine and methamidoxime prodrug **III** (Pafuramidine) (Fig. 1) performed very potent inhibitory activity against protozoan parasites [6,7].

These compounds that bind to DNA do not directly kill the parasite, but cause inhibition of DNA-dependent enzymes or direct inhibition of transcription. Lately, aromatic diguanidine derivatives, which are bioisosteres of amidines, have also been reported to show significant antiprotozoal activity [8–10]. Dicationic compounds such as bisguanidine and bis(2-aminoimidazoline) DNA minor groove binders (Fig. 2) showed *in vitro* activity against *T.b. rhodesiense* and *P. falciparum* at nanomolar concentrations [11].

Our previous studies have shown that not only dicationic compounds but also monocationic compounds exhibited good inhibitory activity against protozoan parasites. Among them, compounds **IV** [12] and **V-VI** [13] (Fig. 3) have significant inhibitory activity against *P. falciparum*. In addition, compounds **V** and **VI** show a good inhibitory activity profile against *T.b. rhodesiense*.

We now report the *in vitro* antiprotozoal evaluation of new monocationic guanidinobenzimidazoles against *P. falciparum*, *T.b. rhodesiense*, *T.cruzi*, *L. donovani* and their molecular docking studies. *In silico* molecular docking analysis was performed to investigate how the compounds interacted with DNA and molecular dynamics simulations were performed to measure the stability and energy of the DNA-ligand complex formed. Besides, theoretical computational ADME study of the compounds was carried out.

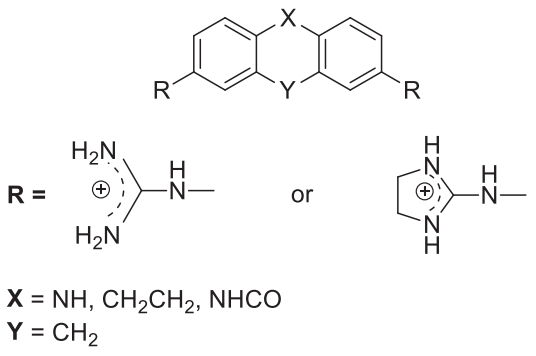

Fig. 2. Dicationic bisguanidine and bis(2-aminoimidazoline) compounds.

2. Material and methods

2.1. Chemistry

Compounds **4**–**23** (Table 1) were prepared using the methods outlined in Scheme 1. 2-Nitro-1,4-phenylenediamine was converted into HCl salt **(1)** with 4 M HCl (in dioxane), stirring at room temperature in ethanol. **1** was reacted with cyanamide to obtain 1-(4-amino-3-nitrophenyl)guanidine HCl **(2)**. Reduction of **2** with H_2/Pd–C afforded 1-(3,4-diaminophenyl)guanidine HCl **(3)**. Cyclization of **3** with sodium metabisulfite ($Na_2S_2O_5$) adduct of corresponding substituted aldehydes gave targeted guanidinobenzimidazoles **(4**–**23)**. HCl salts of compounds were prepared in ethanol with HCl gas.

2.1.1. Experimental

Uncorrected melting points were measured on a Büchi B-540 capillary melting point apparatus. ^{1}H (400 MHz) and ^{13}C (100 MHz) NMR spectra were recorded employing a Varian Mercury 400 MHz FT spectrometer, chemical shifts (δ) are in ppm relative to TMS, and coupling constants (J) are reported in Hertz. Mass spectra were taken on a Waters Micromass ZQ connected with Waters Alliance HPLC, using ESI (+) method, with C-18 column. Elemental analyses were performed by Leco CHNS-932. The compounds reported as salts frequently analyzed correctly for fractional moles of water and/or organic solvent of solvation.

Because of the tautomeric effect of the imidazole ring, the ^{1}H NMR spectra of some compounds was not clear enough, therefore in order to eliminate the tautomerism compounds were dissolved in DMSO-d_6, followed by a tiny amount of dry NaH and 2–3 drops of D_2O were added to NMR tubes and stirred well. In case of any turbidity, the tubes were centrifuged. Clear NMR spectra were observed as reported in the experimental part.

Table 1
Formulas and *in vitro* antiprotozoal activities of **4-23.**

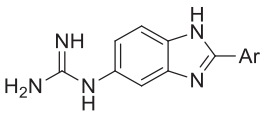

No	Ar	IC50 (μg/mL) [SI]				
		P.f.[a]	*T.b.r.*[a]	*T.c.*[a]	*L.d.*[a]	Cytotoxicity L6 cells[a]
4		4.07	11.6	61.2	>100	>100
5	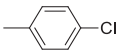	1.89	29.5	90.5	64.5	71.1
6	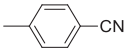	1.17	18.2	89.5	>100	>100
7	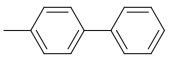	0.018 [2360]	21.5 [2]	54.3 [0.8]	52.55 [0.8]	42.6
8	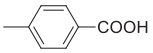	37.2	72.1	59.1	>100	>100
9	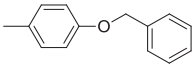	0.226	13.6	38	>100	43.2
10	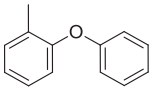	1.87	16.1	49.5	>100	51.6
11	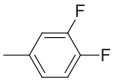	2.67	6.04	67	>100	>100
12	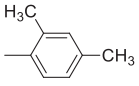	6.26	40.8	62	>100	97.8
13	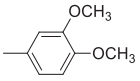	0.153	23.8	>100	>100	78
14	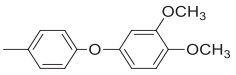	0.052 [>1920]	12.5 [>8]	58.6 [>2]	58 [>2]	>100
15		1.41	11.8	63.6	>100	48.9
16	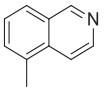	2.72	3.8	8.57	46.3	44.6
17	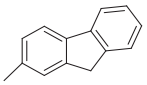	0.168	6.03	34.3	40.3	43.6
18	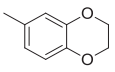	0.82	10.1	75.1	56.2	73.5
19		0.57	12.1	53.1	58.6	40

(*continued on next page*)

Table 1 (*continued*)

No	Ar	IC50 (μg/mL) [SI]				
		P.f.[a]	*T.b.r.*[a]	*T.c.*[a]	*L.d.*[a]	Cytotoxicity L6 cells[a]
20	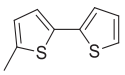	0.19	11.8	46.1	37.7	49.9
21	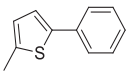	0.279	16	36.5	44	48.4
22	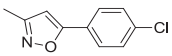	1.14	5.62	21.7	7.7	46.8
23		3.03	17.3	64	90.2	93
Chl.		0.003	-	-	-	-
Mel.		-	0.003	-	-	-
Bnz.		-	-	0.757	-	-
Mil.		-	-	-	0.555	-
Pod.		-	-	-	-	0.006

[a] Activities represent the mean of at least two independent experiments; IC_{50} values used to calculate the average for a given compound were within a factor of two. *P.f.*: *Plasmodium falciparum* NF54, *T.b.r.*: *Trypanosoma brucei rhodesiense* STIB900, *T.c.*: *Trypanosoma cruzi* Tulahuen C4, *L.d.*: *Leishmania donovani* MHOM-ET-67/L82, Chl: Chloroquine, Mel: Melarsoprol, Bnz: Benznidazole, Mil: Miltefosine, Pod: Podophyllotoxin, SI: Selectivity index (IC_{50} L6 cell/IC_{50} parasites).

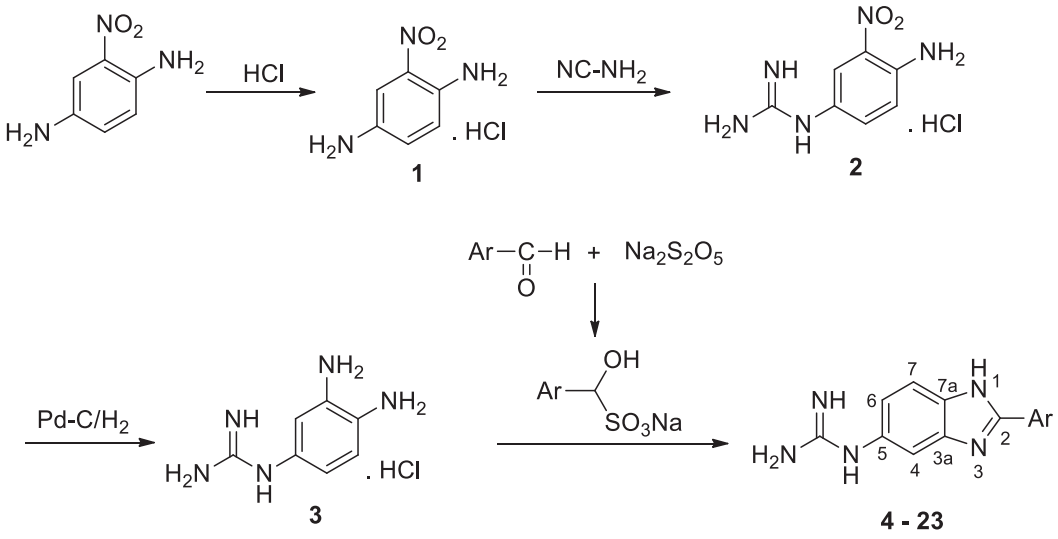

Scheme 1. Synthesis of targeted guanidinobenzimidazoles.

2.1.1.1. 2-Nitro-1,4-phenylenediamine HCl (1). 2-Nitro-1,4-phenylenediamine (2.1 g, 13.7 mmol) was dissolved in 35 mL anhydrous ethanol. 4 M HCl in dioxane (3 mL, 12.3 mmol) was added and stirred at room temperature for 15 min. Diethylether (100 mL) was added, the precipitate was collected by filtration and dried [14]. Yield: 79% (2.57 g), MS (ESI+) *m/z*: 154 (M+H, 100%).

2.1.1.2. 1-(4-Amino-3-nitrophenyl)guanidine HCl (2). The mixture of 1 (1.5 g, 7.9 mmol), cyanamide (2.5 g, 59.5 mmol) and water (0.5 mL) were heated at 60 °C for 1.5 h. It was cooled to room temperature. The excess of diethylether was added slowly, the precipitate was collected by filtration and dried [14]. Yield: 73% (1.09 g). Mp: 170–174 °C, MS (ESI+)*m/z*: 196 (M+H, 100%).

2.1.1.3. 1-(3,4-Diaminophenyl)guanidine HCl (3). The mixture of 2 (0.5 g, 2.16 mmol), Pd–C (10%, 0.046 g), tetrahydrofuran (4.2 mL) and methanol (10 mL) were subjected to hydrogenation using 40 psi of H_2 until the end of H_2 uptake. The catalyst was filtered on a bed of Celite, washed with ethanol and concentrated in vacuo. Powder residue was used for the subsequent steps without crystallization [14]. Yield 93% (0.4 g). Mp: 230–233 °C, MS (ESI+) *m/z*: 166 (M+H, 100%).

2.1.1.4. General synthesis of sodium metabisulfite adduct of substituted aldehydes. Related substituted aldehydes (30 mmol) were dissolved in EtOH (100 mL) and sodium metabisulfite (3.2 g) (in 5 mL of water) was added in portions. The reaction mixture was stirred vigorously. The mixture was kept in a refrigerator for a while. The white precipitate was gained by filtration, dried and

used for the further steps without purification and characterisation.

2.1.1.5. General synthesis of monocationic guanidinobenzimidazole derivatives (4–23). The mixture of 3 (1 mmol) and $Na_2S_2O_5$ adduct of substituted aldehydes (1.1 mmol) in DMF (1 mL) were heated at 100 °C, for 2 h [15]. The reaction mixture was cooled, poured into diluted Na_2CO_3 solution, stirred for a while. The resulting precipitate was collected by filtration washed with water and dried. If the product was not solid, it was extracted with CH_2Cl_2: MeOH (95 : 5). Crystallization or colon chromatography was used for purification. HCl salts of compounds were made in ethanol with HCl gas.

2.1.1.5.1. 1-(2-Phenyl-1H-benzimidazole-5(6)-yl)guanidine HCl (4). Prepared from **3** and $Na_2S_2O_5$ adduct of benzaldehyde (0.23 g) as described in general method. Resulting precipitate was purified with column chromatography using (CH_2Cl_2: MeOH: NH_4OH 50 : 30: 5) as eluant. Crude product was converted to HCl salt, yield 51%, mp > 300 °C. **^{1}H-NMR** δ ppm (DMSO-d_6 + NaH + D_2O): 6.91 (dd, 1H, J = 8 & 1.6 Hz, H-6), 7.29 (d, 1H, J = 1.6 Hz, H-4), 7.44–7.53 (m, 3H, 2-phenyl protons), 7.56 (d, 1H, J = 8.8 Hz, H-7), 8.13 (d, 2H, J = 7.6 Hz, 2-phenyl protons). **COSY**: [H-6: H-7], [H-2′,6': H-3′,5'], [H-4': H-3′, 5']. **^{13}C-NMR** & **HSQC** δ ppm (DMSO-d_6 + NaH + D_2O): 155.7, 152.9, 140.2, 138.4, 134.5, 130.6, 130.4, 129.5, 126.9, 120.3 (CH-6), 116.5 (CH-7), 111.2 (CH-4). **MS** (ESI+) *m/z*: 252 (M+H, 100%). Anal Calcd for $C_{14}H_{13}N_5 \cdot 2HCl \cdot 3H_2O$: C, 44.45; H, 5.59; N, 18.51. Found: C, 44.10; H, 5.44; N, 18.97.

2.1.1.5.2. 1-(2-(4-Chlorophenyl)-1H-benzimidazole-5(6)-yl)guanidine HCl (5). Prepared from **3** and $Na_2S_2O_5$ adduct of 4-chlorobenzaldehyde (0.27 g) as described in general method. Resulting precipitate was purified with column chromatography using (CH_2Cl_2: Isopropanol: NH_4OH 50 : 30: 5) as eluant. Crude product was converted to HCl salt, yield 60%, mp: 175–179 °C. **^{1}H-NMR** δ ppm (DMSO-d_6 + NaH + D_2O): 6.38 (dd, 1H, J = 8.8 & 2 Hz, H-6), 6.91 (d, 1H, J = 2 Hz, H-4), 7.28 (d, 1H, J = 8.8 Hz, H-7), 7.35 (d, 2H, J = 8.8 Hz, 2-phenyl protons), 8.21 (d, 2H, J = 8.8 Hz, 2-phenyl protons). **^{13}C-NMR** & **HSQC** δ ppm (DMSO-d_6 + NaH + D_2O): 158.6, 153.8, 148.1, 143.6, 139.7, 136.8, 131.1, 128.35, 128.3, 116.35 (CH-7), 115.7 (CH-6), 109.9 (CH-4). **MS** (ESI+) *m/z*: 286 (M+H, 33%), 143 (100%), 288 (M+H+2, 11%). Anal Calcd for $C_{14}H_{12}ClN_5 \cdot 2HCl \cdot 4.5H_2O$: C, 38.24; H, 5.27; N, 15.92. Found: C, 38.35; H, 4.60; N, 15.98.

2.1.1.5.3. 1-(2-(4-Cyanophenyl)-1H-benzimidazole-5(6)-yl)guanidine (6). Prepared from **3** and $Na_2S_2O_5$ adduct of 4-cyanobenzaldehyde (0.26 g) as described in general method. The resulting precipitate was crystallised from MeOH, yield 41%, mp > 300 °C. **^{1}H-NMR** δ ppm (DMSO-d_6 + NaH + D_2O): 6.64 (dd, 1H, J = 8.4 & 2.4 Hz, H-6), 7.10 (d, 1H, J = 1.6 Hz, H-4), 7.44 (d, 1H, J = 8 Hz, H-7), 7.81 (d, 2H, J = 8.4 Hz, H-3′,5′), 8.35 (d, 2H, J = 8.4 Hz, H-2′,6′). **COSY**: [H-6: H-7], [H-2′,6': H-3′,5']. **^{13}C-NMR** & **HSQC** & **HMBC** δ ppm (DMSO-d_6 + NaH + D_2O): 155.7 (C-2), 154.3 (C-guanidine), 145.1 (C-3a), 142.8 (C-7a), 139.6 (C-1′), 135.3 (C-5), 132.2 (CH-3′,5′), 126.6 (CH-2′,6′), 119.4 (CN), 117.35 (CH-6), 116.8 (CH-7), 110.6 (CH-4), 108.9 (C-4'). **MS** (ESI+) *m/z*: 277 (M+H, 100%). Anal Calcd for $C_{15}H_{12}N_6 \cdot 2.5H_2O \cdot 0.5CH_3OH$: C, 55.18; H, 5.67; N, 24.91. Found: C, 55.57; H, 5.55; N, 25.33.

2.1.1.5.4. 1-(2-([1,1′-Biphenyl]-4-yl)-1H-benzimidazole-5(6)-yl) guanidine HCl (7). Prepared from **3** and $Na_2S_2O_5$ adduct of 4-phenylbenzaldehyde (0.31 g) as described in general method. Resulting precipitate was purified with column chromatography using (CH_2Cl_2: Isopropanol: NH_4OH 50 : 50: 10) as eluant. Crude product was converted to HCl salt, yield 66%, mp > 300 °C. **^{1}H-NMR** δ ppm (DMSO-d_6 + NaH + D_2O): 6.39 (dd, 1H, J = 8.4 & 2 Hz, H-6), 6.91 (d, 1H, J = 2 Hz, H-4), 7.29 (d, 1H, J = 8.4 Hz, H-7), 7.35 (t, 1H, J = 7.6 Hz, H-4''), 7.48 (t, 2H, J = 7.6 Hz, H-3'',5''), 7.64 (d, 2H, J = 8.4 Hz, 2-phenyl protons), 7.72 (d, 2H, J = 6.8 Hz, H-2'',6''), 8.30 (d, 2H, J = 8.4 Hz, 2-phenyl protons). **COSY**: [H-6: H-7], [H-2′,6': H-3′,5'], [H-2'',6'': H-3'',5''] [H-4'': H-3'',5'']. **^{13}C-NMR** & **HSQC** δ ppm (DMSO-d_6 + NaH + D_2O): 159.4, 153.8, 148.15, 143.7, 140.7, 139.4, 138.2, 137.1, 129.5 (CH-3'',5''), 127.55 (CH-4''), 127.35, 126.7 (CH-2'',6''), 126.6, 116.25, 115.5, 109.9 (CH-4). **MS** (ESI+) *m/z*: 328 (M+H, 45%), 164 (100%). Anal Calcd for $C_{20}H_{17}N_5 \cdot 2HCl \cdot H_2O$: C, 57.42; H, 5.05; N, 16.74. Found: C, 57.54; H, 4.71; N, 16.78.

2.1.1.5.5. 4-(5(6)-Guanidino-1H-benzimidazole-2-yl)benzoic acid (8). Prepared from **3** and $Na_2S_2O_5$ adduct of 4-carboxybenzaldehyde (0.28 g) as described in general method. The resulting precipitate was crystallised from MeOH, yield 73%, mp > 300 °C. **^{1}H-NMR** δ ppm (DMSO-d_6 + NaH + D_2O): 6.46 (dd, 1H, J = 8.4 & 2 Hz, H-6), 6.98 (d, 1H, J = 2.4 Hz, H-4), 7.36 (d, 1H, J = 8.8 Hz, H-7), 7.86 (d, 2H, J = 8.4 Hz, 2-phenyl protons), 8.15 (d, 2H, J = 8.4 Hz, 2-phenyl protons). **COSY**: [H-6: H-7], [H-2′,6': H-3′,5']. **^{13}C-NMR** & **HSQC** δ ppm (DMSO-d_6 + NaH + D_2O): 172.7, 160.2, 154.9, 148.2, 143.9, 139.8, 138.8, 137.5, 129.95, 126.4, 116.9 (H-7), 116.45 (H-6), 110.5 (H-4). **MS** (ESI+) *m/z*: 296 (M+H, 100%). Anal Calcd for $C_{15}H_{13}N_5O_2 \cdot 3.5H_2O$: C, 50.25; H, 5.62; N, 19.54. Found: C, 49.85; H, 5.55; N, 19.17.

2.1.1.5.6. 1-(2-(4-(Benzyloxy)phenyl)-1H-benzimidazole-5(6)-yl) guanidine HCl (9). Prepared from **3** and $Na_2S_2O_5$ adduct of 4-benzyloxybenzaldehyde (0.35 g) as described in general method. The resulting precipitate was purified with column chromatography using (CH_2Cl_2: MeOH: NH_4OH 50 : 20: 2.5) as eluant. Crude product converted to HCl salt, yield 48%, mp: 245–247 °C. **^{1}H-NMR** δ ppm (DMSO-d_6 + NaH + D_2O): 5.13 (s, 1H, C$\underline{H_2}$), 6.35 (dd, 1H, J = 8 & 2 Hz, H-6), 6.90 (d, 1H, J = 1.6 Hz, H-4), 6.97 (d, 2H, J = 8.8 Hz, H-3′,5′), 7.26 (d, 1H, J = 8.4 Hz, H-7), 7.33–7.36 (m, 1H, H-4''), 7.40–7.43 (m, 2H, H-3'',5''), 7.48 (d, 2H, J = 6.8 Hz, H-2'',6''), 8.14 (d, 2H, J = 8.8 Hz, H-2′,6′). **COSY**: [H-6: H-7], [H-3′,5': H-2′,6'], [3'',5'': 2'',6''], [H-4'': H-3'',5'']. **NOESY**: [C$\underline{H_2}$: H-2'',6''(strong) ve H-3′,5'(weak)]. **^{13}C-NMR** δ ppm (DMSO-d_6 + NaH + D_2O): 159.9, 157.7, 154.1, 148.05, 143.7, 138.7, 137.8, 131.0, 128.9, 128.3, 128.1, 115.8, 114.9, 114.7, 109.8, 69.7. **MS** (ESI+) *m/z*: 358 (M+H, 100%). Anal Calcd for $C_{21}H_{19}N_5O \cdot 2HCl \cdot 1.8H_2O$: C, 54.50; H, 5.35; N, 15.13. Found: C, 54.64; H, 5.25; N, 15.25.

2.1.1.5.7. 1-(2-(2-Phenoxyphenyl)-1H-benzimidazole-5(6)-yl)guanidine HCl (10). Prepared from **3** and $Na_2S_2O_5$ adduct of 4-phenoxybenzaldehyde (0.33 g) as described in general method. The resulting precipitate was purified with column chromatography using (CH_2Cl_2: MeOH: NH_4OH 50 : 30: 4) as eluant. Crude product was converted to HCl salt, yield 78%, mp: 290–293 °C. **^{1}H-NMR** δ ppm (CD_3OD): 7.01 (d, 1H, J = 8 Hz), 7.24–7.27 (m, 2H), 7.30–7.35 (m, 1H), 7.40–7.44 (m, 1H), 7.48–7.55 (m, 3H), 7.66–7.71 (m, 1H), 7.820–7.825 (m, 1H), 7.95 (d, 1H, J = 8.8 Hz), 8.18–8.21 (m, 1H). **^{13}C-NMR** δ ppm (CD_3OD): 158.75, 158.4, 155.8, 149.0, 136.85, 134.9, 133.5, 131.9, 131.6, 131.5, 127.0, 125.8, 124.85, 122.2, 118.5, 116.6, 113.6, 112.6. **MS** (ESI+) *m/z*: 344 (M+H, 22%), 172 (100%). Anal Calcd for $C_{20}H_{17}N_5O \cdot 2HCl \cdot 1.5H_2O$: C, 54.18; H, 5.00; N, 15.79. Found: C, 53.73; H, 4.45; N, 15.88.

2.1.1.5.8. 1-(2-(3,4-Difluorophenyl)-1H-benzimidazole-5(6)-yl) guanidine HCl (11). Prepared from **3** and $Na_2S_2O_5$ adduct of 3,4-difluorobenzaldehyde (0.27 g) as described in general method. The resulting precipitate was purified with column chromatography using (CH_2Cl_2: MeOH: NH_4OH 50 : 40: 5) as eluant. Crude product was converted to HCl salt, yield 28%, mp > 300 °C. **^{1}H-NMR** δ ppm (DMSO-d_6 + NaH + D_2O): 6.39 (dd, 1H, J = 8 & 2 Hz, H-6), 6.91 (d, 1H, J = 1.6 Hz, H-4), 7.28 (d, 1H, J = 8.4 Hz, H-7), 7.28–7.35 (m, 1H, 2-phenyl proton), 7.95–7.99 (d, 1H, 2-phenyl proton), 8.03–8.09 (m, 1H, 2-phenyl proton). **COSY**: [H-6: H-7]. **MS** (ESI+) *m/z*: 288 (M+H, 82%), 144 (100%). Anal Calcd for $C_{14}H_{11}F_2N_5 \cdot 2HCl \cdot CH_3OH$: C, 45.93; H, 4.36; N, 17.85. Found: C, 45.67; H, 4.32; N, 17.60.

2.1.1.5.9. 1-(2-(2,4-Dimethylphenyl)-1H-benzimidazole-5(6)-yl) guanidine HCl (12). Prepared from **3** and $Na_2S_2O_5$ adduct of 2,4-dimethylbenzaldehyde (0.26 g) as described in general method.

The resulting precipitate was purified with column chromatography using (CH_2Cl_2: MeOH: NH_4OH 50 : 20: 6) as eluant. Crude product was converted to HCl salt, yield 54%, mp: 215–220 °C (bubling). **^{1}H-NMR** δ ppm (DMSO-d_6 + NaH + D_2O): 2.25 (s, 3H, C$\underline{H}_3$), 2.55 (s, 3H, C$\underline{H}_3$), 6.33 (dd, 1H, J = 8 & 1.6 Hz), 6.90–6.95 (m, 3H), 7.27 (d, 1H, J = 8.4 Hz), 7.73 (d, 1H, J = 7.2 Hz). **^{13}C-NMR** δ ppm (DMSO-d_6 + NaH + D_2O): 161.4, 154.1, 147.6, 143.35, 138.3, 136.2, 135.3, 135.0, 131.4, 130.6, 126.1, 115.95, 114.7, 109.9, 22.2, 21.1. **MS** (ESI+) *m/z*: 280 (M+H, 100%). Anal Calcd for $C_{16}H_{17}N_5 \cdot 2HCl \cdot 0.5C_2H_5OH$: C, 54.40; H, 5.90; N, 18.66. Found: C, 54.05; H, 6.37; N, 18.66.

2.1.1.5.10. 1-(2-(3,4-Dimetoxyphenyl)-1H-benzimidazole-5(6)-yl) guanidine HCl (13). Prepared from **3** and $Na_2S_2O_5$ adduct of 2,4-dimethoxybenzaldehyde (0.3 g) as described in general method. The resulting precipitate was crystallised from MeOH. Crude product was converted to HCl salt, yield 50%, mp: 285–289 °C (bubling). **^{1}H-NMR** δ ppm (DMSO-d_6 + NaH + D_2O): 3.77 (s, 3H, C$\underline{H}_3$), 3.84 (s, 3H, C$\underline{H}_3$), 6.32 (dd, 1H, J = 8 & 2 Hz, H-6), 6.87 (d, 1H, J = 2 Hz, H-4), 6.90 (d, 1H, J = 8.4 Hz, H-5′), 7.23 (d, 1H, J = 8 Hz, H-7), 7.76 (dd, 1H, J = 8 & 2 Hz, H-6′), 7.90 (d, 1H, J = 2 Hz, H-2′). **COSY**: [H-6: H-7], [H-5': H-6']. **^{13}C-NMR** & **HSQC** δ ppm (DMSO-d_6 + NaH + D_2O): 160.0, 153.85, 148.55, 148.1, 147.9, 143.7, 138.9, 131.2, 119.0 (CH-6′), 115.7, 114.8 (CH-6), 111.8 (CH-5′), 110.7 (CH-2'), 109.6 (CH-4), 55.9 (OCH_3), 55.7 (OCH_3). **MS** (ESI+) *m/z*: 312 (M+H, 38%), 156 (100%). Anal Calcd for $C_{16}H_{17}N_5O_2 \cdot 2HCl \cdot 2.5H_2O$: C, 44.76; H, 5.63; N, 16.77. Found: C, 44.85; H, 4.94; N, 16.35.

2.1.1.5.11. 1-(2-(4-(3,4-Dimetoxyphenoxy)phenyl)-1H-benzimidazole-5(6)-yl)guanidine HCl (14). Prepared from **3** and $Na_2S_2O_5$ adduct of 4-(3,4-Dimethoxyphenoxy)benzaldehyde (0.4 g) as described in general method. The resulting precipitate was purified with column chromatography using (CH_2Cl_2: MeOH: NH_4OH 50 : 30: 5) as eluant. Crude product was converted to HCl salt, yield 40%, mp: 230–234 °C. **^{1}H-NMR** δ ppm (CD_3OD): 3.79 (s, 3H, 3''-OC$\underline{H}_3$), 3.83 (s, 3H, 4''-OC$\underline{H}_3$), 6.63 (dd, 1H, J = 8.4 & 1.2 Hz, H-6''), 6.76 (d, 1H, J = 2.8 Hz, H-2''), 6.97 (d, 1H, J = 8.4 Hz, H-5''), 7.06 (d, 2H, J = 8.4 Hz, H-3′,5′), 7.14 (dd, 1H, J = 8.4 & 1.6 Hz, H-6), 7.51 (d, 1H, J = 1.6 Hz, H-4), 7.63 (d, 1H, J = 8.4 Hz, H-7), 8.04 (d, 2H, J = 8.8 Hz, H-2′,6′). **COSY**: [H-6: H-7], [H-2′,6': H-3′,5'], [H-5'': H-6'']. **NOESY**: [3''-OC$\underline{H}_3$: H-2''], [4''-OC$\underline{H}_3$: H-5'']. **^{13}C-NMR** & **HSQC** & **HMBC** δ ppm (CD_3OD): 162.3(C-2), 158.6 (C-guanidine), 154.9 (C-4′), 151.8 (C-3''), 150.95 (C-1''), 147.7 (C-4''), 130.7 (C-5), 129.75 (CH-2′,6′), 124.6 (C-1′), 122.3 (CH-6), 118.65 (CH-3′,5′), 113.95 (CH-5''), 112.9 (CH-6''), 106.5 (CH-2''), 57.0 (4''-OCH_3), 56.6 (3''-OCH_3). **MS** (ESI+) *m/z*: 404 (M+H, 60%), 202 (100%). Anal Calcd for $C_{22}H_{21}N_5O_3 \cdot 2HCl \cdot 6H_2O$: C, 45.21; H, 6.03; N, 11.98. Found: C, 45.22; H, 5.13; N, 12.37.

2.1.1.5.12. 1-(2-(Naphthalene-1-yl)-1H-benzimidazole-5(6)-yl) guanidine (15). Prepared from **3** and $Na_2S_2O_5$ adduct of 1-Naphthylbenzaldehyde (0.29 g) as described in general method. The resulting precipitate was purified with column chromatography using (CH_2Cl_2: MeOH: NH_4OH 50 : 30: 5) as eluant, yield 45%, mp: 280–286 °C (bubling). **^{1}H-NMR** δ ppm (DMSO-d_6 + NaH + D_2O): 6.41 (dd, 1H, J = 8.4 & 2 Hz, H-6), 6.99 (d, 1H, J = 2 Hz, H-4), 7.37 (d, 1H, J = 8.4 Hz, H-7), 7.45–7.53 (m, 3H), 7.79 (d,1H, J = 8.4 Hz), 7.86–7.89 (m, 1H), 8.15 (dd, 1H, J = 7.2 & 1.2 Hz), 9.51–9.53 (m,1H). **COSY**: [H-6: H-7]. **^{13}C-NMR** δ ppm (DMSO-d_6 + NaH + D_2O): 160.7, 153.8, 147.9, 143.65, 139.1, 135.8, 134.1, 131.7, 129.0, 128.0, 127.6, 126.8, 125.8, 125.5, 116.3, 115.1, 109.9. **MS** (ESI+) *m/z*: 302 (M+H, 52%), 151 (100%). Anal Calcd for $C_{18}H_{15}N_5 \cdot 4H_2O \cdot 0.2CH_3OH$: C, 48.19; H, 4.39; N, 15.43. Found: C, 47.90; H, 4.25; N, 15.13.

2.1.1.5.13. 1-(2-(Isoquinoline-5-yl)-1H-benzimidazole-5(6)-yl) guanidine HCl (16). Prepared from **3** and $Na_2S_2O_5$ adduct of isoquinoline-5-carboxyaldehyde (0.29 g) as described in general method. The resulting precipitate was purified with column chromatography using (CH_2Cl_2: MeOH: NH_4OH 50 : 30: 5) as eluant. Crude product was converted to HCl salt, yield 30%, mp: 205–210 °C. **^{1}H-NMR** δ ppm (DMSO-d_6 + NaH + D_2O): 6.41 (dd, 1H, J = 8 & 2 Hz, H-6), 6.98 (d, 1H, J = 2 Hz, H-4), 7.37 (d, 1H, J = 8 Hz, H-7), 7.67 (t, 1H, J = 8 Hz, H-7′), 7.97 (d, 1H, J = 8.4 Hz), 8.43 (d, 1H, J = 6.4 Hz), 8.46 (dd, 1H, J = 7.6 & 1.2 Hz, H-3′), 9.22 (s, 1H, H-1′), 9.48 (d, 1H, J = 6 Hz, H-4′). **COSY**: [H-6: H-7], [H-3': H-4'], [H-6': H-7'], [H-7': H-8']. **^{13}C-NMR** & **HSQC** δ ppm (DMSO-d_6 + NaH + D_2O): 159.5, 153.9, 152.6 (CH-1′), 148.1, 143.7, 142.5, 139.7, 134.4, 134.0, 131.4 (CH-3′), 129.6, 127.7 (CH_2-7′), 126.6, 121.9 (CH-4'), 116.7 (CH-7), 115.75 (CH-6), 110.2 (CH-4). **MS** (ESI+) *m/z*: 303 (M+H, 40%), 152 (100%). Anal Calcd for $C_{17}H_{14}N_6 \cdot 3HCl \cdot 4H_2O$: C, 42.20; H, 5.20; N, 17.37. Found: C, 42.58; H, 4.84; N, 17.73.

2.1.1.5.14. 1-(2-(9H-fluorene-2-yl)-1H-benzimidazole-5(6)-yl) guanidine HCl (17). Prepared from **3** and $Na_2S_2O_5$ adduct of fluorene-2-carboxyaldehyde (0.33 g) as described in general method. The resulting precipitate was purified with column chromatography using (CH_2Cl_2: MeOH: NH_4OH 50 : 30: 3) as eluant. Crude product was converted to HCl salt, yield 14%, mp > 300 °C. **^{1}H-NMR** δ ppm (DMSO-d_6 + NaH + D_2O): 4.05 (s, 2H, C$\underline{H}_2$), 7.21 (dd, 1H, J = 8.4 & 2 Hz, H-6), 7.35–7.45 (m, 2H), 7.56 (d, 1H, J = 2 Hz), 7.64 (d, 1H, J = 7.2 Hz), 7.74 (d, 1H, J = 8 Hz, H-7), 7.97 (d, 1H, J = 7.6 Hz), 8.09 (d, 1H, J = 8.4 Hz), 8.20 (d, 1H, J = 8 Hz), 8.36 (s, 1H). **COSY**: [H-6: H-7]. **^{13}C-NMR** δ ppm (DMSO-d_6 + NaH + D_2O): 156.9, 152.2, 146.1, 145.1, 144.9, 140.4, 135.8, 134.15, 131.9, 129.2, 128.1, 127.3, 126.25, 124.7, 123.7, 123.6, 121.7, 116.2, 112.3, 37.3. **MS** (ESI+) *m/z*: 340 (M+H, 82%), 170 (100%). Anal Calcd for $C_{21}H_{17}N_5 \cdot 2HCl \cdot 1.5H_2O$: C, 57.41; H, 5.04; N, 15.94. Found: C, 57.30; H, 5.05; N, 16.32.

2.1.1.5.15. 1-(2-(1,4-Benzodioxane-6-yl)-1H-benzimidazole-5(6)-yl)guanidine HCl (18). Prepared from **3** and $Na_2S_2O_5$ adduct of 1,4-benzodioxane-6-carboxyaldehyde (0.3 g) as described in general method. The resulting precipitate was purified with column chromatography using (CH_2Cl_2: MeOH: NH_4OH 50 : 20: 1) as eluant. Crude product was converted to HCl salt, yield 11%, mp > 300 °C. **^{1}H-NMR** δ ppm (DMSO-d_6 + NaH + D_2O): 4.22 (br.s, 4H, C$\underline{H}_2$, overlapped water peak), 6.30 (dd, 1H, J = 8.4 & 2 Hz, H-6), 6.75 (dd, 1H, J = 8.8 Hz, H-8′), 6.84 (d, 1H, J = 2 Hz, H-4), 7.20 (d, 1H, J = 8.4 Hz, H-7), 7.66–7.68 (m, 2H, H-5′,7′). **COSY**: [H-6: H-7], [H-7': H-8']. **^{13}C-NMR** & **HSQC** δ ppm (DMSO-d_6 + NaH + D_2O): 159.6, 153.8, 148.0, 143.6, 143.1, 142.5, 138.7, 131.8, 120.05, 116.6 (CH-8'), 115.7 (CH-7), 115.3, 114.7 (CH-6), 109.6 (CH-4), 64.5, 64.4. **MS** (ESI+) *m/z*: 310 (M+H, 65%), 155 (100%). Anal Calcd for $C_{16}H_{15}N_5O_2 \cdot 2HCl \cdot 2H_2O$: C, 45.94; H, 5.06; N, 16.74. Found: C, 45.54; H, 5.03; N, 17.06.

2.1.1.5.16. 1-(2-(Benzo[b]thiophene-3-yl)-1H-benzimidazole-5(6)-yl)guanidine HCl (19). Prepared from **3** and $Na_2S_2O_5$ adduct of benzo[*b*]thiophene-3-carboxyaldehyde (0.29 g) as described in general method. The resulting precipitate was purified with column chromatography using (CH_2Cl_2: MeOH: NH_4OH 50 : 30: 3) as eluant. Crude product was converted to HCl salt, yield 35%, mp > 300 °C. **^{1}H-NMR** δ ppm (DMSO-d_6 + NaH + D_2O): 6.39 (dd, 1H, J = 8.4 & 2.4 Hz, H-6), 6.95 (d, 1H, J = 2 Hz, H-4), 7.32–7.44 (m, 3H, H-7,5′,6′), 7.91 (d, 1H, J = 8 Hz, H-4′), 8.07 (s, 1H, H-2′), 9.11 (d, 1H, J = 7.6 Hz, H-7′). **COSY**: [H-6: H-7], [H-4': H-5'], [H-5': H-6'], [H-6': H-7']. **^{13}C-NMR** & **HSQC** & **HMBC** δ ppm (DMSO-d_6 + NaH + D_2O): 157.5 (C-2), 154.3 (C-guanidine), 147.6 (C-5), 143.3 (C-7a), 140.5 (C-3'a), 139.3 (C-3a), 138.5 (C-7'a), 134.7 (C-3′), 126.7 (CH-7′), 124.6 (CH-5′,6′), 123.7 (CH-2′), 122.9 (CH-4′), 116.4 (CH-7), 115.6 (CH-6), 110.1 (CH-4). **MS** (ESI+) *m/z*: 308 (M+H, 42%), 154 (100%). Anal Calcd for $C_{16}H_{13}N_5S \cdot 2HCl \cdot 2.5H_2O$: C, 45.18; H, 4.73; N, 16.46; S, 7.53. Found: C, 45.62; H, 4.002; N, 16.78; S, 7.90.

2.1.1.5.17. 1-(2-([2,2′-Bithiophene]-5-yl)-1H-benzimidazole-5(6)-yl)guanidine HCl (20). Prepared from **3** and $Na_2S_2O_5$ adduct of 2,2′-bithiophene-5-carboxyaldehyde (0.33 g) as described in general method. The resulting precipitate was purified with column chromatography using (CH_2Cl_2: MeOH: NH_4OH 60 : 30: 2) as eluant. Crude product was converted to HCl salt, yield 25%, mp > 300 °C.

^{1}H-NMR δ ppm (D_2O): 6.83 (s, 1H, H-4''), 6.84 (d, 1H, J = 4 Hz), 6.98 (dd, 1H, J = 3.6 & 1.2 Hz), 7.04 (dd, 1H, J = 8.8 & 2 Hz, H-6), 7.15 (d, 1H, J = 2 Hz, H-4), 7.24 (dd, 1H, J = 5.2 & 1.2 Hz), 7.34 (s, 1H, H-7), 7.37 (d, 1H, J = 4 Hz). **COSY**: [H-6: H-7], [H-3': H-4'], [H-3'': H-4''], [H-4'': H-5'']. **^{13}C-NMR** δ ppm (D_2O): 158.9, 148.45, 146.2, 137.6, 137.15, 135.5, 134.75, 133.9, 131.2, 129.8, 128.5, 127.2, 126.4, 124.9, 117.7, 112.9. **MS** (ESI+) *m/z*: 340 (M+H, 100%). Anal Calcd for $C_{16}H_{13}N_5S_2 \cdot 2HCl \cdot 2.5H_2O$: C, 42.01; H, 4.40; N, 15.31; S, 14.02. Found: C, 41.92; H, 3.98; N, 15.22; S, 14.31.

2.1.1.5.18. 1-(2-(5-Phenylthiophene-2-yl)-1H-benzimidazole-5(6)-yl)guanidine HCl (21). Prepared from **3** and $Na_2S_2O_5$ adduct of 5-phenylthiophene-2-carboxyaldehyde (0.32 g) as described in general method. The resulting precipitate was purified with column chromatography using (CH_2Cl_2: MeOH: NH_4OH 50 : 30: 1) as eluant. Crude product was converted to HCl salt, yield 41%, mp: 200–204 °C (bubling). **^{1}H-NMR** δ ppm (DMSO-d_6 + NaH + D_2O): 6.40 (dd, 1H, J = 8.4 & 2 Hz, H-6), 6.86 (d, 1H, J = 2 Hz, H-4), 7.22–7.26 (m, 2H), 7.36–7.40 (m, 3H), 7.54 (d, 1H, J = 4 Hz), 7.64 (d, 1H, J = 6.8 Hz). **COSY**: [H-6: H-7]. **^{13}C-NMR** δ ppm (DMSO-d_6 + NaH + D_2O): 169.0, 156.1, 154.7, 148.1, 143.7, 142.0, 141.9, 140.1, 135.1, 130.1, 128.2, 125.8, 125.3, 124.9, 116.6, 116.5, 110.2. **MS** (ESI+) *m/z*: 344 (M+H, 61%), 167 (100%). Anal Calcd for $C_{18}H_{15}N_5S \cdot 2HCl \cdot 2.5H_2O$: C, 47.89; H, 4.91; N, 15.51; S, 7.10. Found: C, 48.29; H, 4.77; N, 15.90; S, 6.69.

2.1.1.5.19. 1-(2-(5-(4-Chlorophenyl)isoxazole-3-yl)-1H-benzimidazole-5(6)-yl)guanidine HCl (22). Prepared from **3** and $Na_2S_2O_5$ adduct of 5-(4-chlorophenyl)isoxazole-3-carboxyaldehyde (0.34 g) as described in general method. The resulting precipitate was purified with column chromatography using (CH_2Cl_2: MeOH: NH_4OH 50 : 20: 2) as eluant. Crude product was converted to HCl salt, yield 34%, mp: 241–246 °C (bubling). **^{1}H-NMR** δ ppm (CD_3OD): 7.56 (d, 1H, J = 2 Hz, H-6), 7.58–7.61 (m, 3H), 7.84 (d, 1H, J = 1.6 Hz, H-4), 7.95–7.97 (m, 3H). **COSY**: [H-6: H-7], [H-2'',6'': H-3'',5'']. **^{13}C-NMR** δ ppm (CD_3OD): 173.4, 158.4, 152.7, 142.7, 138.75, 135.3, 134.7, 132.9, 130.85, 128.85, 126.3, 126.0, 117.3, 113.1, 100.4. **MS** (ESI+) *m/z*: 353 (M+H, 100%), 355 (M+H+2, 34%). Anal Calcd for $C_{17}H_{13}ClN_6O \cdot 2HCl \cdot 2H_2O$: C, 44.22; H, 4.14; N, 18.20. Found: C, 43.78; H, 4.12; N, 18.33.

2.1.1.5.20. 1-(2-(4-Methylthiazole-5-yl)-1H-benzimidazole-5(6)-yl)guanidine HCl (23). Prepared from **3** and $Na_2S_2O_5$ adduct of 4-methylthiazole-5-carboxyaldehyde (0.25 g) as described in general method. The resulting precipitate was crystallised from EtOH. Crude product was converted to HCl salt, yield 70%, mp: 265–270 °C (bubling). **^{1}H-NMR** δ ppm (CD_3OD): 2.82 (s, 3H, -C$\underline{H}_3$), 7.57 (dd, 1H, J = 9.2 & 2 Hz, H-6), 7.83 (d, 1H, J = 1.6 Hz, H-4), 7.95 (d, 1H, J = 9.2 Hz, H-7), 9.45 (s, 1H, H-2'). **COSY**: [H-6: H-7]. **^{13}C-NMR** & **HSQC** & **HMBC** δ ppm (CD_3OD): 160.3 (CH-2'), 159.2 (C-5'), 158.4 (C-guanidine), 145.0 (C-2), 135.2 (C-5), 133.8 (C-3a), 132.2 (C-7a), 126.1 (CH-6), 116.7 (CH-7), 115.4 (C-4'), 112.6 (CH-4), 16.9 (4'-CH_3). **MS** (ESI+) *m/z*: 273 (M+H, 100%). Anal Calcd for $C_{12}H_{12}N_6S \cdot 2HCl \cdot 4H_2O$: C, 34.53; H, 5.31; N, 20.13; S, 7.68. Found: C, 34.53; H, 4.41; N, 19.70; S, 8.05.

2.2. Biology

2.2.1. Antiprotozoal activity

In vitro assays with *P. falciparum* NF54, *T.b. rhodesiense* STIB900, *T. cruzi* Tulahuen C4 and *L. donovani* MHOM-ET-67/L82 were carried out as previously reported [16].

2.2.2. Cytotoxicity studies

Cytotoxicity was evaluated using cultured L-6 rat myoblast cells and an Alamar Blue assay as previously reported [16].

2.3. Computational details

2.3.1. Molecular docking

The molecular docking studies were carried out using Glide implemented in the Schrödinger Small-Molecule Drug Discovery Suite (Small-Molecule Drug Discovery Suite 2020-2, Schrödinger, LLC, New York, NY, 2020). The compounds which were built via builder panel in Maestro were subjected to ligand preparation by LigPrep (Schrödinger Release 2020-2: LigPrep, Schrödinger, LLC, New York, NY, 2020) using default conditions. The x-ray crystal structure of DB819-d(CGCGAATTCGCG)$_2$ complex (PDB code: 3OIE) [17] was retrieved from the Protein Data Bank. The protein was prepared using the Protein Preparation Wizard tool. Water molecules and metal ions were deleted and hydrogen atoms were added followed by the assignment of all atom charges and atom types. Finally, energy minimization and refinement of the structures were done up to 0.3 Å RMSD by applying the OPLS3e force field. The centroid of the x-ray ligand was defined as the grid box. van der Waals (vdW) radius scaling factor 1.00, partial charge cutoff 0.25, and OPLS3e force filed were used for receptor grid generation. The docking protocol was validated by a RMSD value of 1.22 which was predicted by superimposing the bioactive conformation of x-ray ligand and its redocked conformation. The compounds prepared by LigPrep were docked into DNA using the extra-precision (XP) docking mode of the Glide without any constraints and a 0.75 vdW radius scaling factor and 0.15 partial charge cutoff [18]. The protocol facilitates docking by ligand flexibility and generation of multiple conformers within the rigid receptor. The best conformation for each compound was chosen based on the lowest XP glide score.

2.3.2. Molecular dynamics

Molecular dynamics simulations study was performed using GROMACS 2020.4 [19] version (GROningen MAChine for Chemical Simulations). The DNA topology file was created using the Amber99sb-ildn force field [20] and the TIP3P water model was used. The topology file of compounds **7** and **14** were created via ACPYPE Server [21] (https://www.bio2byte.be/acpype/) by selecting bond charge correction (BCC) charge method and general Amber force field (GAFF) atom type and net charge +1. Three separate system files were created for DNA apo form, DNA-compound **7** and **14** holo forms. Systems were solvated using Simple Point Charge water (SPC) 216 and 21 Na^+ were added to equilibrate the systems charges. System energy was minimized, 10 ns duration canonical ensemble (amount of substance (N), pressure (P) and temperature (T) - NPT) and isothermal-isobaric (amount of substance (N), volume (V) and equilibrium steps temperature (T) - NVT) stages were performed, and 200 ns duration molecular dynamics simulations were performed. RMSD, RMSF and intermolecular hydrogen bond analyzes were performed. Finally, the average interaction energy between protein and ligand was calculated according to short-range Lennard-Jones energy. The results were monitored using Visual Molecular Dynamics (VMD) [22] and trajectory graphs were created with QtGrace tools.

2.3.3. Theoretical ADME calculations

Computational analysis was performed using SwissADME (http://www.swissadme.ch/) to estimate the physicochemical properties, pharmacokinetic properties and ADME parameters of the compounds [23].

3. Results and discussion

3.1. Antiparasitic activity evaluation

All targeted guanidinobenzimidazole compounds **4**–**23**

(Table 1), were tested *in vitro* in serial drug dilution assays for antiparasitic activity against *P. falciparum*, *T.b. rhodesiense*, *T. cruzi* and *L. donovani*. Cytotoxicity of the synthesized compounds was determined using the Alamar Blue assay with rat skeletal myoblasts (L6 cells). Based on the outcomes of this *in vitro* study these compounds seem to have no cytotoxicity liability. The IC_{50} values of the compounds against *P. falciparum* ranged from 0.018 to 37.15 μg/mL (Table 1). Best inhibitory activity against *P. falciparum* were obtained with **7** (IC_{50} = 0.018 μg/mL and SI = 2360) and **14** (IC_{50} = 0.052 μg/mL and SI > 1920) which are possessing biphenyl and 4-(3,4-dimethoxyphenoxy)phenyl groups at C-2 position, respectively. In addition, compounds **13**, **17** and **20** also showed good inhibitory activity with the IC_{50} values of 0.153, 0.168 and 0.19 μg/mL, respectively. The common feature of these molecules is that they all possess bulky aromatic rings such as biphenyl, 4-(3,4-dimethoxy-phenoxy)phenyl, fluorene and bithiophene at the C-2 position of benzimidazole moiety.

The inhibitory effect of the tested molecules against the trypanosomatid parasites was moderate at best. Three compounds, **11** (IC_{50} = 6.04 μg/mL), **16** (IC_{50} = 3.8 μg/mL) and **22** (IC_{50} = 5.62 μg/mL) exhibited moderate activity against *T.b. rhodesiense* and one compound, **16** (IC_{50} = 8.57 μg/mL) against *T. cruzi*. None of the tested compounds was active against *L. donovani*.

3.2. Molecular docking studies

To predict the preferred orientation of compounds **7** and **14** inside the DNA, molecular docking studies were performed. The obtained results indicated that both compounds bound in the minor groove of the d(CGCGAATTCGCG)$_2$ duplex. The resulting lowest binding energies for **7** and **14** were found to be −9.372 kcal/mol and −9.764 kcal/mol, respectively. The orientation of **7** allowed to stack with the center of the DNA minor groove covering almost five base pairs. The protonated guanidine moiety extended towards from the groove, leading the NH groups to be closer to DNA phosphate moiety and favorably interacted with G22 via salt bridge interaction and H-bonding. The NH moiety of benzimidazole ring involved in H-bonding with T19 while the aromatic H-bondings were also observed formed with T7, T8, T19, and T20 base pairs enhancing the complex stability. In the case of **14**, a similar binding conformation was observed to that of **7**, but slightly bended compared to **7**. Compound **14** occupied the region of about six base pairs in DNA minor groove interacting with the single monomer of the DNA structure via H-bonding between the guanidine and carbonyl oxygen of C21 and between the N1 hydrogen of the benzimidazole ring and the carbonyl oxygen of T19. On the other hand, the aromatic H-bondings with T7, T8 and C9 carbonyl oxygens through the aromatic hydrogens of phenyl rings were also observed allowing interaction with the other monomer of the DNA structure (Fig. 4).

3.3. Molecular dynamics simulations

Molecular dynamics simulations are the basic computational method used in drug design and development processes to measure the interaction stability and energy of small molecule lead compounds with biological macromolecular molecules such as protein, DNA and RNA [24,25]. To monitor the behavior of the DNA-ligand complex formed by the protozoal DNA of compounds **7** and **14** obtained by molecular docking under *in silico* physiological conditions and to calculate the stability due to time, a molecular dynamic simulation of 200 ns was performed. Also, ligand-free DNA was simulated in the environment, conditions and time to ensure the reliability of the created molecular dynamics system and to detect the changes caused by the interaction of compounds **7** and

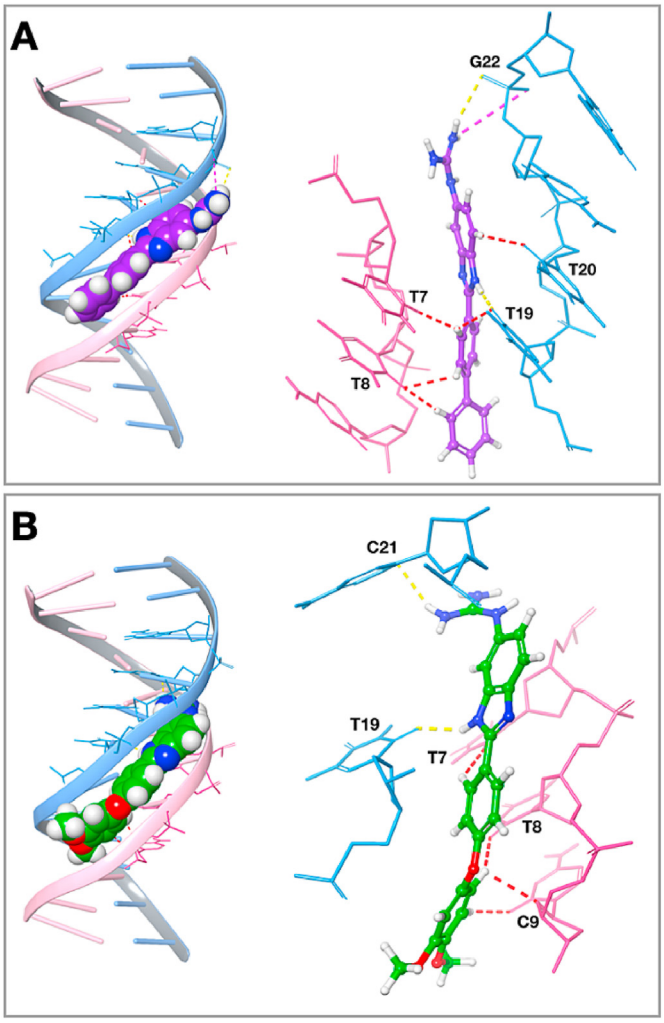

Fig. 4. Predicted binding modes of compounds **7** (A) and **14** (B) in DNA structure (PDB code: 3OIE). Dashed-yellow lines represent hydrogen bonds and dashed-red lines represent aromatic hydrogen bonds.

14 with DNA. Trajectory analysis of RMSD, RMSF, intermolecular hydrogen bond and protein-ligand interaction was performed. RMSD measurements are the main parameters used to measure protein-DNA stability and deviations in molecular dynamics simulations [26]. As shown in Fig. 5a, the RMSD values of the apo form (3OIE-Apo), compounds **7** (3OIE-LIG7) and **14** (3OIE-LIG14) holo forms were measured below 0.5 nm 3OIE-Apo, 3OIE-LIG7 and 3OIE-LIG14 gave an average RMSD value of 0.294 nm, 0.334 nm and 0.283 nm, respectively. The interaction of compounds **7** and **14** with DNA did not cause a significant change in stability. The deviation of the ligands during the 200 ns simulation period was also analyzed. As shown in Fig. 5b, compound **7** measured a small deflection of less than 0.1 nm during 130 ns and an RMSD value of less than 0.15 after 130 ns. Compound **14** showed deviations below 0.15 nm up to 60 ns, RMSD value up to 0.25 nm between 60 and 110 ns and a fluctuating value below 0.15 nm after 110 ns.

Another important parameter is the RSMF calculation used to measure the fluctuation and conformational change of macromolecules [27]. As an indicator of the stability and binding strength of the ligand, it should reduce the fluctuation of the residues with which it interacts at the active site and increases its stability. RMSF analysis performed based on residue is given in Fig. 5c for 3OIE-Apo, 3OIE-LIG7, and 3OIE-LIG14. Besides, in Fig. 6, the 2D diagram

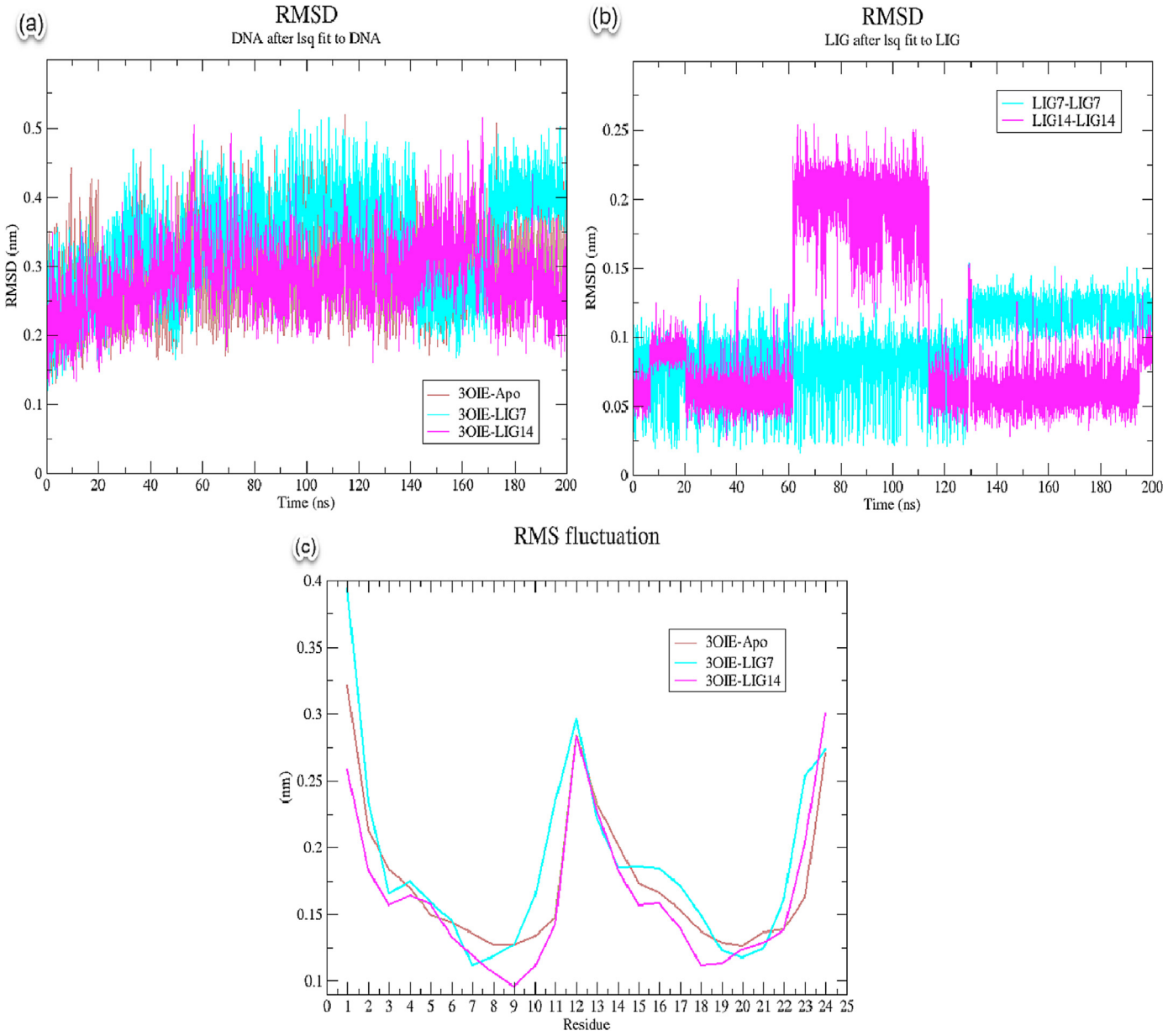

Fig. 5. (a) DNA-root mean square deviation (RMSD), (b) Ligand-RMSD and (c) root mean square fluctuation (RMSF), analysis of the apo form (3OIE-Apo), compounds **7** (3OIE-LIG7) and **14** (3OIE-LIG14) holo forms of protozoal DNA throughout 200 ns.

of the DNA-ligand interactions obtained with Glide XP at the DNA active site of compounds **7** and **14** is presented. When the RMSF graph and the 2D DNA-ligand interaction diagram are evaluated together, the base pairs T19 and G22 of B chain in which they form hydrogen bonds show less fluctuation than the apo form and it is understood to make it more stable. Compound **14**, on the other hand, gave lower RMSF values compared to the apo form in T19 and C21 base pairs of B chain which are involved in hydrogen bonding was formed and the DNA became more stable.

The presence and number of hydrogen bonds in protein-ligand or DNA-ligand interactions could indicate that the ligand will interact more with the macromolecule and form a more stable complex [28]. Therefore, the time-dependent number and change of hydrogen bonds were analyzed. As shown in Fig. 7a, during the 200 ns simulation, compound **7** often formed two hydrogen bonds, sometimes three hydrogen bonds and occasionally four hydrogen bonds. As shown in Fig. 7b, compound **14** frequently formed four to five hydrogen bonds. Besides hydrogen bond analysis, the Lennard-Jones DNA-ligand interaction energy was measured over time. Lennard-Jones energy is an energy measurement method that is widely used in molecular dynamics simulations to calculate the interaction energies of molecules that are not directly bonded but are standing together [29]. As given in Fig. 7c, the 3OIE-LIG7 complex produced approximately −150 kJ mol^{-1} to 175 kJ mol^{-1}, while 3OIE-LIG14 produced −175 kJ mol^{-1} to −250 kJ mol^{-1} DNA ligand binding energy, respectively. −167.75 kJ mol^{-1} and -220.671 kJ mol^{-1} average short-range Lennard-Jones gave energy values.

3.4. Computational ADME estimations

Many drug molecule candidates do not have suitable

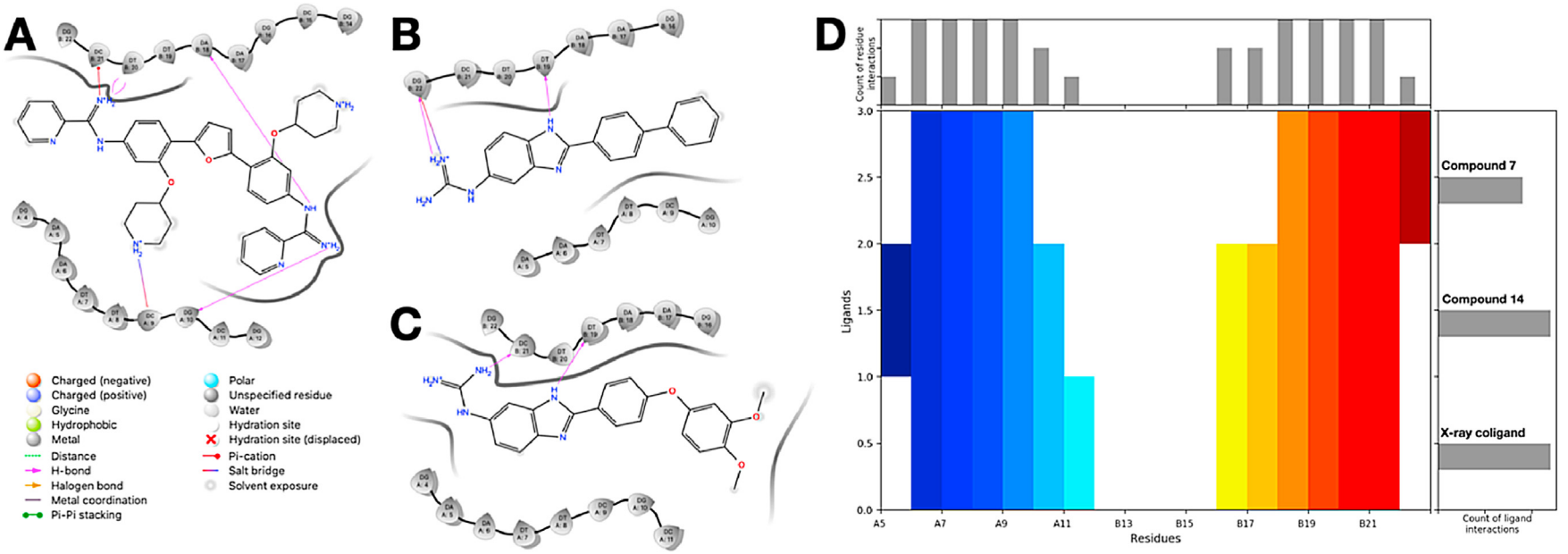

Fig. 6. 2D Schematic diagram describing the DNA-ligand interactions obtained with Glide XP at the DNA active site of (A) x-ray ligand, compounds (B) **7** and (C) **14** (PDB ID: 3OIE). (D) The interaction fingerprint matrix that identifying the binding patterns of compounds with DNA (PDB ID: 3OIE).

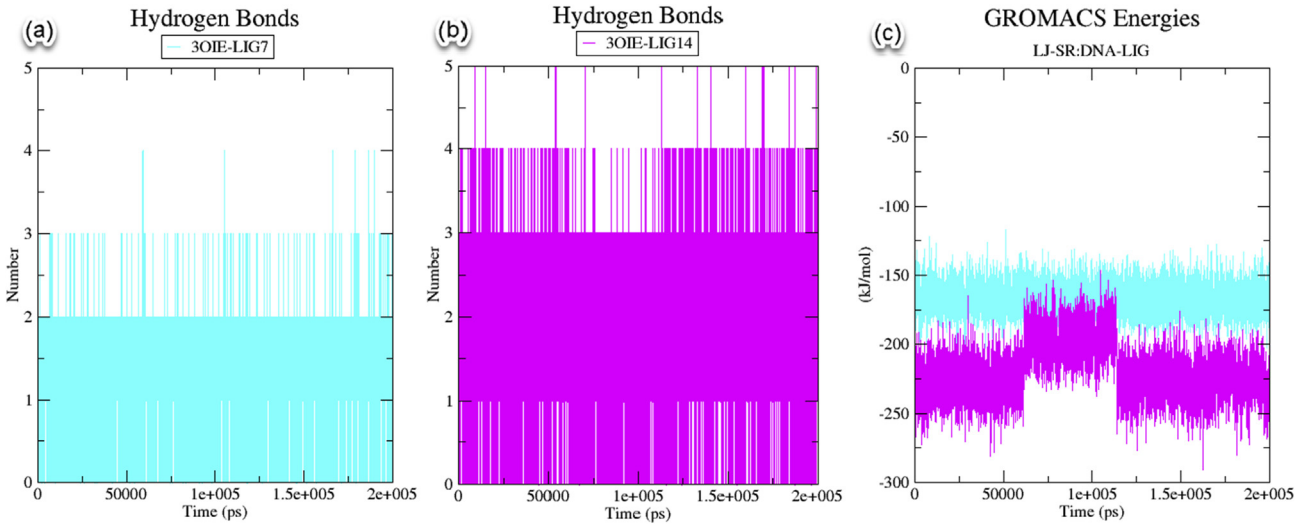

Fig. 7. (a, b) Intermolecular H bonds number between protozoal DNA and compounds **7**–**14**, (c) the short-range Lennard-Jones DNA-ligand interaction energy for 200 ns (PDB ID: 3OIE).

pharmacokinetic properties, although they show active properties during phase studies, they fail to succeed. For this reason, it is beneficial to calculate some computational and predictable parameters. Molecular weight, number of rotatable bonds, hydrogen acceptors, hydrogen donors, molar refractivity, and octanol/water partition coefficient were calculated. Lipinski and Ghose were evaluated according to the restrictive rules. According to Lipinski's rule of 5, MW $\leq$ 500, MLogP $\leq$4.15, N or O $\leq$ 10 and NH or OH $\leq$ 5 [30], according to Ghose's rule, 160 $\leq$ MW $\leq$ 480, $-0.4 \leq$ WLogP $\leq$ 5.6, 40 $\leq$ MR $\leq$ 130 and 20 $\leq$ atoms $\leq$ 70 [31]. Accordingly, as seen in Table 2, all of the compounds comply with Lipinski's and Ghose's rules. All calculated parameters are given in supporting data. According to theoretical calculations, the ADME parameters of the compounds are within suitable limits.

4. Conclusions

This study indicated that 2-(aryl-substituted-1*H*-benzimidazole-5(6)-yl)guanidine derivatives show a good inhibitory activity profile against *P. falciparum*. Especially, two of them (**7, 14**) showed close activity against *P. falciparum* compared to reference drug chloroquine. It is apparent that substitution of C-2 position with bulky aromatic rings is critical for optimal anti-malarial activity. These compounds also showed moderate activity against *T.b. rhodesiense* as compared to the reference drug melarsoprol. None of the tested compounds exhibited a good activity against *T. cruzi* or *L. donovani*. Molecular docking studies for compounds **7** and **14** supported the biological data indicating that these compounds are interacting DNA through minor groove binding. According to the molecular dynamics study, compounds **7** and **14** remain stable during 200 ns simulation, form 4 to 5 hydrogen bonds and average short-range Lennard-Jones DNA-ligand energy of -167.75 kJ mol^{-1} and -220.67 kJ mol^{-1} form, respectively. *In vivo* studies of

Table 2
Calculated and evaluated SwissADME parameters.

Comp.	MW	#Rotatable bonds	#H-bond acceptors	#H-bond donors	MLogP	WLogP	MR	GI absorption	Lipinski #violations	Ghose #violations
4	251.29	3	2	4	1.92	2.34	77.13	High	0	0
5	285.73	3	2	4	2.45	3.00	82.14	High	0	0
6	276.30	3	3	4	1.29	2.22	81.85	High	0	0
7	327.38	4	2	4	3.15	4.01	102.57	High	0	0
8	295.30	4	4	5	1.31	2.04	84.09	High	0	0
9	357.41	6	3	4	2.83	3.77	108.11	High	0	0
10	343.38	5	3	4	2.88	4.14	103.65	High	0	0
11	287.27	3	4	4	2.72	3.46	77.05	High	0	0
12	279.34	3	2	4	2.43	2.96	87.07	High	0	0
13	311.34	5	4	4	1.35	2.36	90.12	High	0	0
14	403.43	7	5	4	2.27	4.15	116.63	High	0	0
15	301.35	3	2	4	2.73	3.50	94.64	High	0	0
16	302.33	3	3	4	1.68	2.89	92.43	High	0	0
17	339.39	3	2	4	3.38	3.92	105.58	High	0	0
18	309.32	3	4	4	1.35	2.12	88.00	High	0	0
19	307.37	3	2	4	2.55	3.56	92.52	Low	0	0
20	339.44	4	2	4	2.28	4.13	98.32	High	0	0
21	333.41	4	2	4	2.73	4.07	100.45	High	0	0
22	352.78	4	4	4	2.20	3.65	97.64	High	0	0
23	272.33	3	3	4	0.61	2.11	77.77	High	0	0

MW: Molecular weight. #Rotatable bonds: Number of rotatable bonds. #H-bond acceptors: Number of hydrogen acceptors. #H-bond donors: Number of hydrogen donors. MLogP: Topological method - WLogP atomistic method octanol/water partition coefficient. MR: Molar refractivity. GI: Gastrointestinal absorption.

compounds **7** and **14** are in progress, to test efficacy in an animal model of infection and to establish pharmacokinetic profiles.

Declaration of competing interest

The authors declare that they have no known competing financial interests or personal relationships that could have appeared to influence the work reported in this paper.

Acknowledgements

This work was supported by Ankara University Scientific Research Fund (BAP-17L0237006). Central Laboratory of Pharmacy Faculty of Ankara University provided support for acquisition of the NMR, Mass spectrometer and elemental analyzer used in this work. All molecular dynamics simulations reported were performed utilizing TUBITAK (The Scientific and Technological Research Council of Turkey), ULAKBIM (Turkish Academic Network and Information Centre), High Performance and Grid Computing Centre (TRUBA resources).

Appendix A. Supplementary data

Supplementary data to this article can be found online at https://doi.org/10.1016/j.ejmech.2021.113545.

References

[1] WHO neglected tropical diseases. https://www.who.int/neglected_diseases/diseases/en/, 2019. (Accessed 1 October 2019) accessed.
[2] M.N.C. Soeiro, E.M. de Souza, C.E. Stephens, D.W. Boykin, Aromatic diamidines as antiparasitic agents, Expet Opin. Invest. Drugs 14 (8) (2005) 957–972, https://doi.org/10.1517/13543784.14.8.957.
[3] M.S. Bartlett, T.D. Edlind, C.H. Lee, R. Dean, S.F. Queener, M.M. Shaw, J.W. Smith, Albendazole inhibits *Pneumocystis carinii* proliferation in inoculated immunosuppressed mice, Antimicrob. Agents Chemother. 38 (8) (1994) 1834–1837, https://doi.org/10.1128/AAC.38.8.1834.
[4] M.A. Ismail, A. Batista-Parra, Y. Miao, W.D. Wilson, T. Wenzler, R. Brun, D.W. Boykin, Dicationic near-linear biphenyl benzimidazole derivatives as DNA-targeted antiprotozoal agents, Bioorg. Med. Chem. 13 (2005) 6718–6726, https://doi.org/10.1016/j.bmc.2005.07.024.
[5] H. Göker, D.W. Boykin, S. Yıldız, Synthesis and potent antimicrobial activity of some novel 2-phenyl or methyl-4*H*-1-benzopyran-4-ones carrying amidinobenzimidazoles, Bioorg. Med. Chem. 13 (2005) 1707–1714, https://doi.org/10.1016/j.bmc.2004.12.006.
[6] D.W. Boykin, Antimicrobial activity of the DNA minor groove binders furamidine and analogs, J. Braz. Chem. Soc. 13 (6) (2002) 763–771, https://doi.org/10.1590/S0103-50532002000600006.
[7] S. Mallena, M.P.H. Lee, C. Bailly, S. Neidle, A. Kumar, D.W. Boykin, W.D. Wilson, Thiophene-based diamidine forms a "super" AT binding minor groove agent, J. Am. Chem. Soc. 126 (2004) 13659–13669, https://doi.org/10.1021/ja048175m.
[8] C.E. Stephens, R. Brun, M.M. Salem, K.A. Werbovetz, F. Tanious, W.D. Wilson, D.W. Boykin, The activity of diguanidino and 'reversed' diamidino 2,5-diarylfurans versus *Trypanosoma cruzi* and *Leishmania donovani*, Bioorg. Med. Chem. Lett 13 (2003) 2065–2069, https://doi.org/10.1016/S0960-894X(03)00319-6.
[9] R.K. Arafa, R. Brun, T. Wenzler, F.A. Tanious, W.D. Wilson, C.E. Stephens, D.W. Boykin, Synthesis, DNA affinity, and antiprotozoal activity of fused ring dicationic compounds and their prodrugs, J. Med. Chem. 48 (2005) 5480–5488, https://doi.org/10.1021/jm058190h.
[10] P.G. Baraldi, A. Bovero, F. Fruttarolo, D. Preti, M.A. Tabrizi, M.G. Pavani, R. Romagnoli, DNA minor groove binders as potential antitumor and antimicrobial agents, Med. Res. Rev. 24 (4) (2004) 475–528, https://doi.org/10.1002/med.20000.
[11] F. Saczewski, L. Balewski, Biological activities of guanidine compounds, Expert Opin. Ther. Pat. 19 (10) (2009) 1417–1448, https://doi.org/10.1517/13543770903216675.
[12] C. Karaaslan, M. Kaiser, R. Brun, H. Göker, Synthesis and potent antiprotozoal activity of mono/di amidino 2-anilinobenzimidazoles versus *Plasmodium falciparum* and *Trypanosoma brucei rhodesiense*, Bioorg. Med. Chem. 24 (2016) 4038–4044, https://doi.org/10.1016/j.bmc.2016.06.047.
[13] M. Alp, H. Göker, R. Brun, S. Yıldız, Synthesis and antiparasitic and antifungal evaluation of 2'-arylsubstituted-1*H*,1'*H*-[2,5']bisbenzimidazolyl-5-carboxamidines, Eur. J. Med. Chem. 44 (2009) 2002–2008, https://doi.org/10.1016/j.ejmech.2008.10.003.
[14] T.J. Church, N.S. Cutshall, A.R. Gangloff, T.E. Jenkins, M.S. Linsell, J. Litvak, K.D. Rice, J.R. Spencer, V.R. Wang, Compounds and Compositions for Treating Diseases Associated with Serine Protease, Particularly Tryptase, Activity, 1998. WO 98/45275.
[15] H.F. Ridley, R.G.W. Spickett, G.M. Timmis, A new synthesis of benzimidazoles and aza-analogs, J. Heterocycl. Chem. 2 (1965) 453–456, https://doi.org/10.1002/jhet.5570020424.
[16] F.A. Bernal, M. Kaiser, B. Wünsch, T.J. Schmidt, Structure-activity relationships of cinnamate ester analogues as potent antiprotozoal agents, ChemMedChem 15 (1) (2020) 68–78, https://doi.org/10.1002/cmdc.201900544.
[17] Y. Chai, M. Munde, A. Kumar, L. Mickelson, S. Lin, N.H. Campbell, M. Banerjee, S. Akay, Z. Liu, A.A. Farahat, R. Nhili, S. Depauw, M.H. David-Cordonnier, S. Neidle, W.D. Wilson, D.W. Boykin, Structure-dependent binding of arylimidamides to the DNA minor groove, Chembiochem 15 (2014) 68–79, https://doi.org/10.1002/cbic.201300622.
[18] R.A. Friesner, R.B. Murphy, M.P. Repasky, L.L. Frye, J.R. Greenwood, T.A. Halgren, P.C. Sanschagrin, D.T. Mainz, Extra precision glide: docking and scoring incorporating a model of hydrophobic enclosure for protein-ligand complexes, J. Med. Chem. 49 (2006) 6177–6196, https://doi.org/10.1021/jm051256o.
[19] M.J. Abraham, T. Murtola, R. Schulz, S. Pall, J.C. Smith, B. Hess, E. Lindahl, GROMACS: High performance molecular simulations through multi-level parallelism from laptops to supercomputers, SoftwareX 1 (2015) 19–25, https://doi.org/10.1016/j.softx.2015.06.001.
[20] K. Lindorff-Larsen, S. Piana, K. Palmo, P. Maragakis, J.L. Klepeis, R.O. Dror, D.E. Shaw, Improved side-chain torsion potentials for the Amber ff99SB protein force field, Proteins Struct. Funct. Bioinf. 78 (8) (2010) 1950–1958, https://doi.org/10.1002/prot.22711.
[21] A.W.S. da Silva, W.F. Vranken, ACPYPE-Antechamber python parser interface, BMC Res. Notes 5 (1) (2012) 1–8, https://doi.org/10.1186/1756-0500-5-367.
[22] W. Humphrey, A. Dalke, K. Schulten, VMD: visual molecular dynamics, J. Mol. Graph. 14 (1) (1996) 33–38, https://doi.org/10.1016/0263-7855(96)00018-5.
[23] A. Daina, O. Michielin, V. Zoete, SwissADME: a free web tool to evaluate pharmacokinetics, drug-likeness and medicinal chemistry friendliness of small molecules, Sci. Rep. 7 (1) (2017) 1–13, https://doi.org/10.1038/srep42717.
[24] H. Zhao, A. Caflisch, Molecular dynamics in drug design, Eur. J. Med. Chem. 91 (2015) 4–14, https://doi.org/10.1016/j.ejmech.2014.08.004.
[25] P. Śledź, A. Caflisch, Protein structure-based drug design: from docking to molecular dynamics, Curr. Opin. Struct. Biol. 48 (2018) 93–102, https://doi.org/10.1016/j.sbi.2017.10.010.
[26] K. Sargsyan, C. Grauffel, C. Lim, How molecular size impacts RMSD applications in molecular dynamics simulations, J. Chem. Theor. Comput. 13 (4) (2017) 1518–1524, https://doi.org/10.1021/acs.jctc.7b00028.
[27] L. Martínez, Automatic identification of mobile and rigid substructures in molecular dynamics simulations and fractional structural fluctuation analysis, PloS One 10 (3) (2015), e0119264, https://doi.org/10.1371/journal.pone.0119264.
[28] H. Wang, Z. Gao, P. Song, B. Hu, J. Wang, M. Cheng, Molecular dynamics simulation and QM/MM calculation reveal the selectivity mechanism of type I 1/2 kinase inhibitors: the effect of intramolecular H-bonds and conformational restriction for improved selectivity, Phys. Chem. Chem. Phys. 21 (43) (2019) 24147–24164, https://doi.org/10.1039/c9cp04353e.
[29] T. Steinbrecher, D.L. Mobley, D.A. Case, Nonlinear scaling schemes for Lennard-Jones interactions in free energy calculations, J. Chem. Phys. 127 (21) (2007) 214108, https://doi.org/10.1063/1.2799191.
[30] C.A. Lipinski, Lead- and drug-like compounds: the rule-of-five revolution, Drug Discov. Today Technol. 1 (4) (2004) 337–341, https://doi.org/10.1016/j.ddtec.2004.11.007.
[31] A.K. Ghose, V.N. Viswanadhan, J.J. Wendoloski, A knowledge-based approach in designing combinatorial or medicinal chemistry libraries for drug discovery. 1. A qualitative and quantitative characterization of known drug databases, J. Comb. Chem. 1 (1) (1999) 55–68, https://doi.org/10.1021/cc9800071.